

L
568
A21
126
3

VHF OMNIRANGE WAVE REFLECTIONS FROM WIRES

CAA Library

By
S. R. Anderson and H. F. Keary
Electronics Division

Technical Development Report No. 126



CIVIL AERONAUTICS ADMINISTRATION
TECHNICAL DEVELOPMENT AND
EVALUATION CENTER
INDIANAPOLIS, INDIANA

May 1952

TABLE OF CONTENTS

	Page
SUMMARY	1
INTRODUCTION	1
EQUIPMENT	1
TESTS	1
THEORETICAL CONSIDERATIONS	5
CONCLUSIONS	11
APPENDIX I	12
APPENDIX II	16
APPENDIX III	18

Manuscript received September 1950

VHF OMNIRANGE WAVE REFLECTIONS FROM WIRES

SUMMARY

This report presents data obtained both by measurements made on the ground and during flights of a very-high-frequency omnidirectional radio range (VOR) with horizontal wires, metallic fences, and wooden fences located near the station for the purpose of determining their effect on the performance of the omnirange. The phenomena of wave reflections from wires are treated mathematically.

INTRODUCTION

VOR facilities are located at approximately 100-mile intervals so that an aircraft about to fly beyond the distance range of one station will have guidance from the adjacent station without a break in continuity. The proper siting of a large number of stations on a national basis is a difficult task considering the fact that many objects, such as trees, fences, buildings, and wires may have an adverse effect on the omnirange radiation pattern. This report is confined to a study of the effect of nearby fences and overhead horizontal wires on the operation of the VHF omnirange.

EQUIPMENT

A standard VOR facility with a counterpoise 15 feet above ground was used as the test station for all tests except in the case of the long straight fence test where the counterpoise was 10 feet above ground. The antenna array consisted of four loop antennas fed by two VHF bridge circuits. Wooden poles spaced approximately 200 feet apart were used to support either one or two No. 6 solid copper conductors. Fences 100 feet and 50 feet long were built to rotate about a 50-foot vertical wooden pole. A test was conducted at an existing omnirange station where a farmer's fence five feet high and several thousand feet long passed within 50 feet of the VOR antennas.

All observations in flight were made in a Douglas C-47 aircraft carrying a standard VOR receiving installation which included a Collins Type 51R-1 navigation receiver. Ground measurements were made with standard VOR receivers at a number of azimuths from the VOR. The course deviation indicator movements were recorded to permit later analysis.

TESTS

A test was made to simulate the conditions where an overhead power line is brought to the station along a radial direction. A No. 6 copper wire was secured to the edge of the counterpoise and was run radially for a distance of 577 feet, 15 feet above ground. The far end of the wire sloped to the ground for a distance of 200 feet and extended along the ground for approximately 200 feet to simulate an infinite line. Two flights were made around the VOR at radii of 6.9 and 15.0 miles. The results of these flights, when compared with those obtained with the wire removed, indicated that no effects were caused by the radial wire.

The conditions and results of each of the other tests are shown in Figs. 1 to 9, on which the measured course deviation indicator error versus azimuth is plotted.

This information was obtained when flying around the VOR at a constant radius of 15 miles. The omnibearing selector was set every ten degrees so that the aircraft would continually cross the course just selected. A comparison of such recordings, with and without the wire under test, indicates the effect of the wire on the course deviation indicator. The curves show the greatest over-all error in each 10° sector. Over-all error is defined as the difference between the number of degrees traversed by the course deviation indicator (extremes plus to minus) with the test wire in place and with the test wire removed.

A study of Figs. 1 to 9 reveals that

1. The north half of the wire in Figs. 1 to 4, is responsible for the northerly lobe, while the south half is responsible for the southerly lobe. Compare Fig. 4 with Fig. 5.

2. The length of the northerly extension of wire is not critical with regard to error in the 50° to 70° sector so long as the wire is not less than 200 feet in length.

3. Raising the wire from 15 to 30 feet above ground increased the error approximately 90 per cent.

4. The removal of the ground terminations had negligible effect on lobe size, but it did narrow the lobe, thereby reducing the 40° azimuth error.

5. The radial wire shown in Fig. 7 had negligible effect, as may be seen by comparing Figs. 6 and 7.

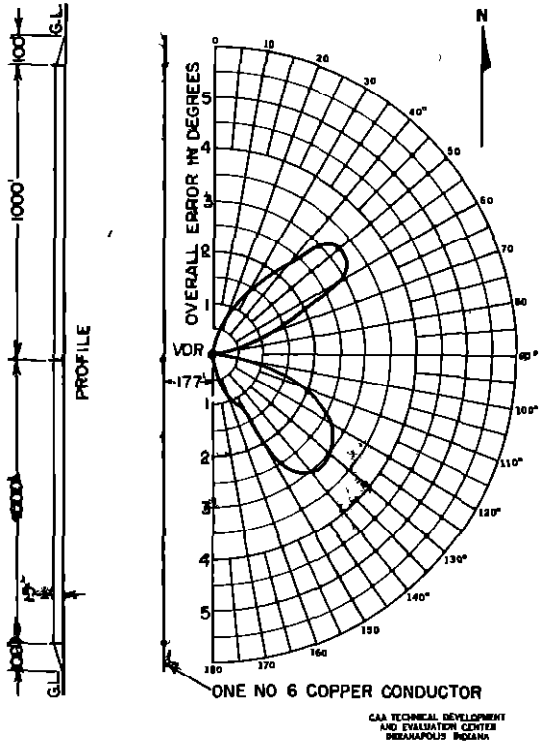


Fig. 1 Measured Course Deviation Indicator Error Versus Azimuth

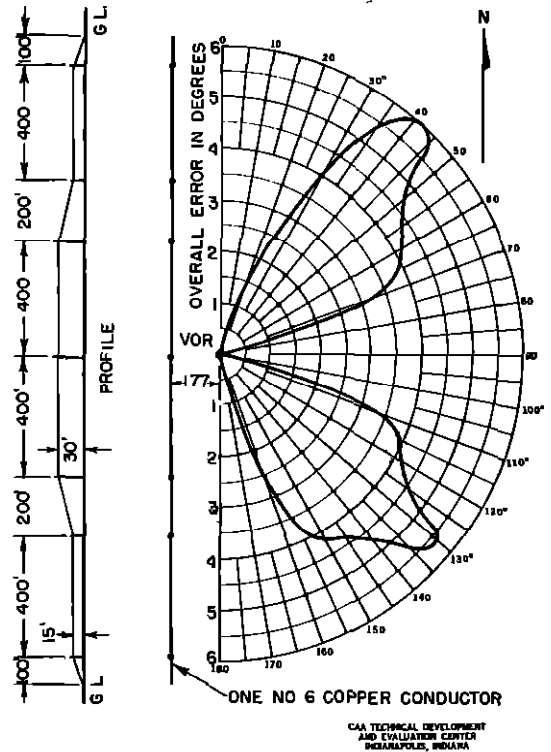


Fig. 2 Measured Course Deviation Indicator Error Versus Azimuth

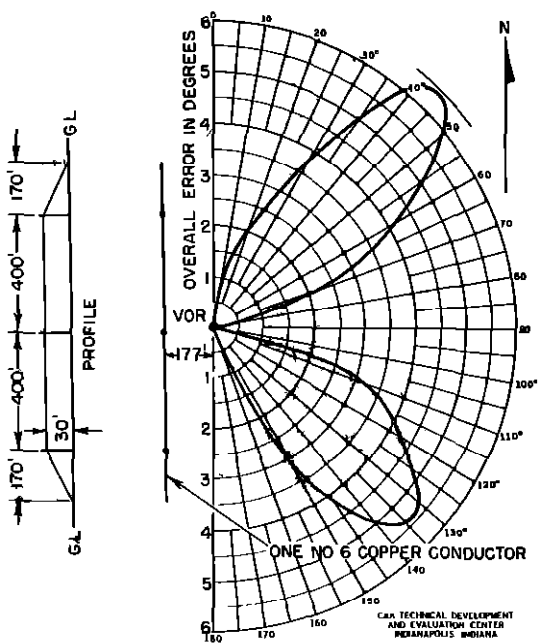


Fig. 3 Measured Course Deviation Indicator Error Versus Azimuth

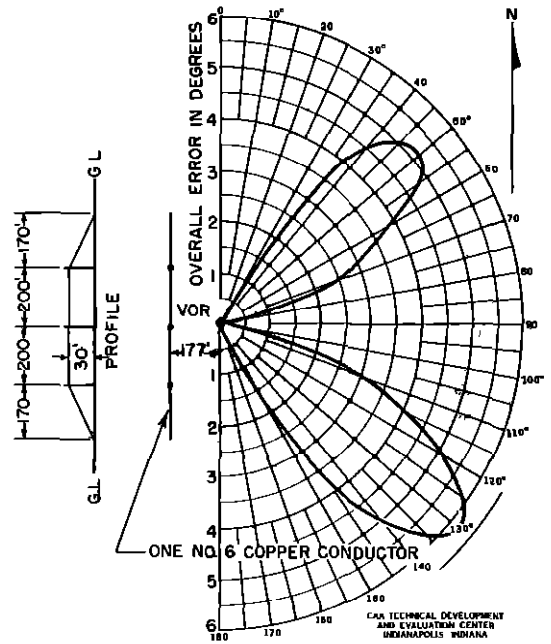


Fig. 4 Measured Course Deviation Indicator Error Versus Azimuth

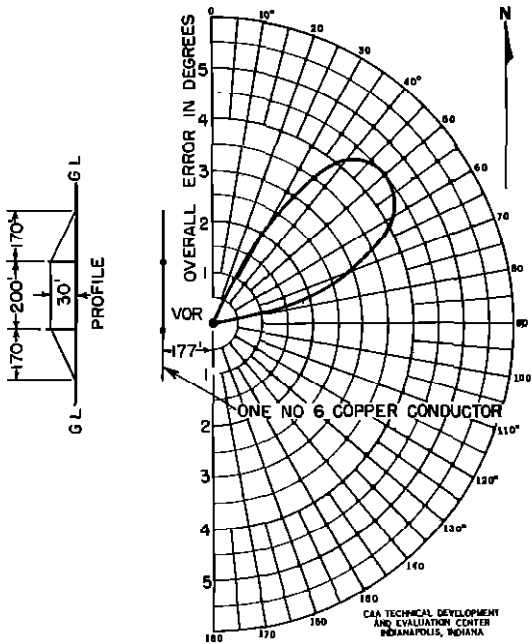


Fig. 5 Measured Course Deviation Indicator Error Versus Azimuth

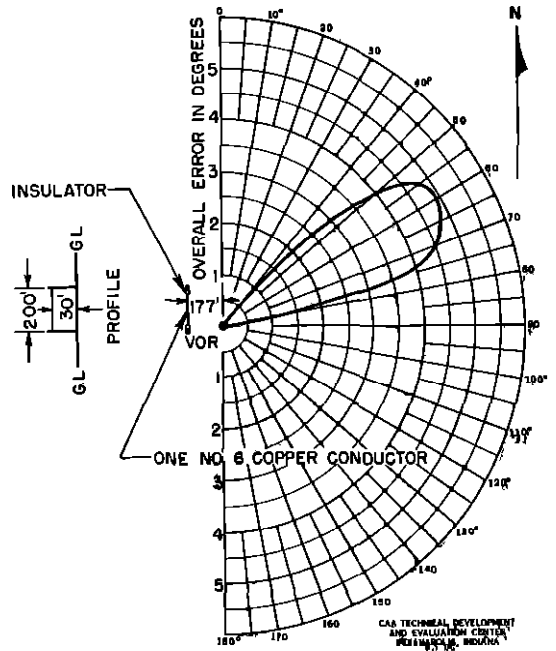


Fig. 6 Measured Course Deviation Indicator Error Versus Azimuth

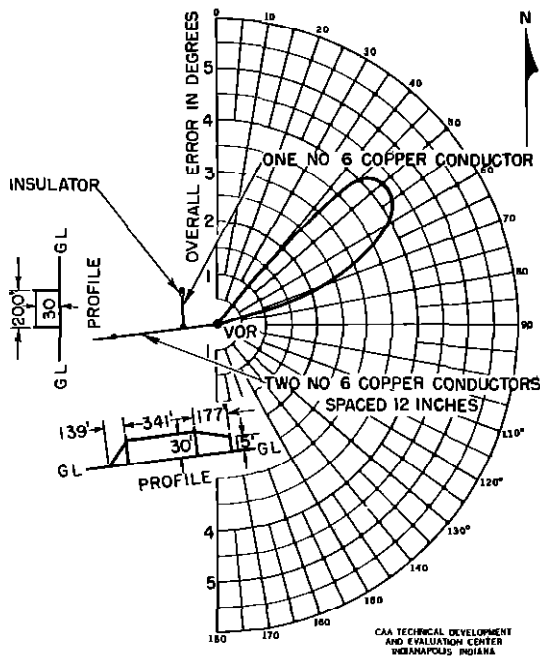


Fig. 7 Measured Course Deviation Indicator Error Versus Azimuth

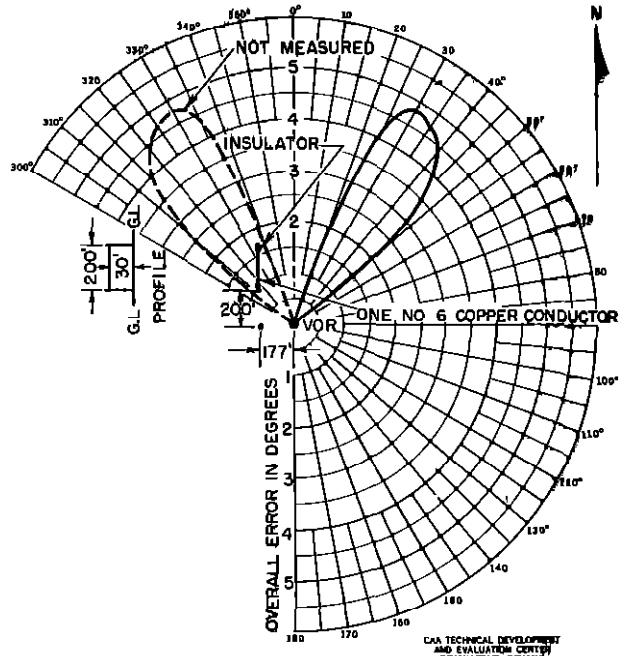


Fig. 8 Measured Course Deviation Indicator Error Versus Azimuth

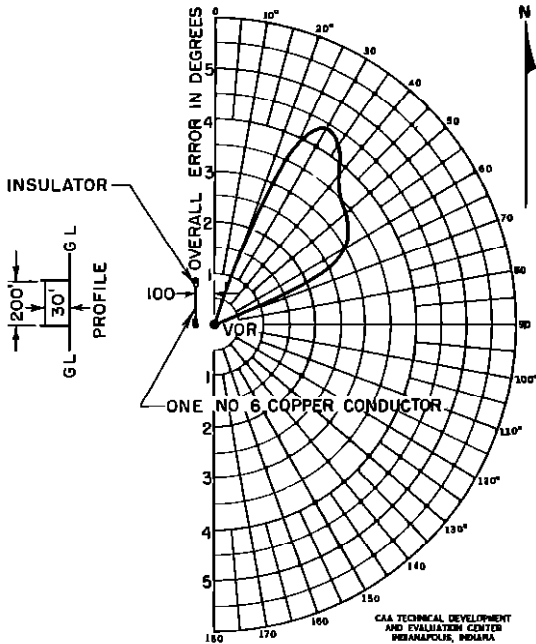


Fig. 9 Measured Course Deviation Indicator Error Versus Azimuth

6 Fig 8 indicates that the lobe points more to the north as the wire is moved to the north. This would be expected from optical reflection theory.

7 Fig 9 shows that moving the wire closer to the VOR produces strong reflections in the directions 30° and 40° azimuth, as does moving the wire to the north. These facts also support optical reflection theory.

The test conditions in Fig 6 were repeated, but instead of one conductor, two No 6 solid copper conductors spaced 12 inches apart were used to determine the effect of a reduced characteristic impedance. Due to the additional wire, approximately 56 per cent increase in error was observed.

In view of the increase in error ex-

perienced by an increase in wire height from 15 to 30 feet and by the use of two conductors 12 inches apart in place of one conductor, the radial wire test was repeated. The additional test was performed with two No 6 solid copper wires spaced 12 inches apart. The wires were fastened 15 feet above ground to the edge of the counterpoise. The wire rose to 30 feet above ground within a distance of 162 feet, then ran 341 feet at 30 feet above ground, and sloped to the ground in the next 139 feet. A number of radial flights and one 15-mile radius circular flight were made, and it was found that the radial wires caused no detectable effect. Theoretically, this should be so since the electric vector radiates from the VOR array, is horizontal, and is everywhere perpendicular to the wires. Therefore, no current could be induced in the wires to produce a radiation field.

A wire fence 100 feet long and 6 feet high was constructed with its midpoint mounted on a vertical pole so that the fence could be rotated about the pole. The center of the fence (supporting pole) was 177 feet from the VOR array which was located on a 15-foot high, 35-foot diameter counterpoise. A VOR receiver with a course deviation indicator recorder attached was located at a number of different azimuths and approximately 2,000 feet from the VOR. A rotation of the fence produced such a small error that it was difficult to measure (approximately 0.5° total spread).

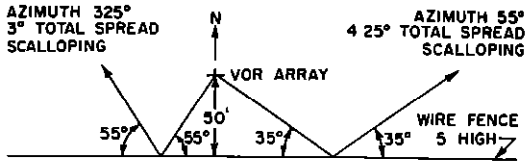
A second test was performed at a VOR having an existing straight-line fence, five feet high and several thousand feet long, and 50 feet from the VOR at the nearest point. Fig 10A displays the situation. Table I shows some of the characteristics of the fence as a reflector with all data, except that marked theoretical, taken from flight records.

The maximum scalloping measured on the east side of the station occurred at an

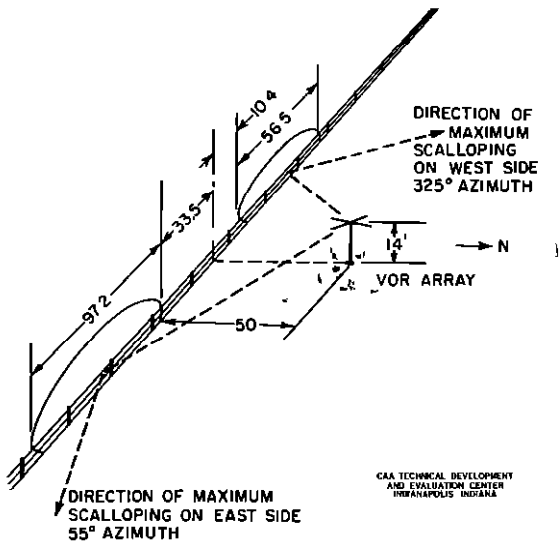
TABLE I

Scalloping Characteristics From a Wire Fence

Azimuth (Degrees)	Radius of Circle Flown (Miles)	Width of Scalloping Sector (Degrees)	Maximum Scalloping Amplitude Total Spread (Degrees)	Scalloping Frequency (cps)	Theoretical Scalloping Frequency (cps)
325	20	10	2.25	0.011	0.014
50	6	10	4.2	0.03	0.04
325	6	10	3.0		



A. Plan View of VOR Array With Respect to the Wire Fence. The Direction and Amplitude of Maximum Measured Scalloping Are Given



B. Parts of Fence Causing Maximum Scalloping, Determined Theoretically

Fig. 10 An Example of a Fence Which Caused Scalloping on a VOR and the Parts of the Fence Causing the Scalloping

angle of reflection of 35°, while the angle of reflection on the west side was 55°. The reason for the difference appears to be due to the ground elevation which is less on the west side of the site than on the east side. The amplitude of the scalloping bears out this explanation, since the scalloping is greater on the east side than on the west side.

The parts of the fence which caused the maximum scalloping were determined by using the directions of maximum scalloping obtained from flight recordings and Equations (14) and (15). The results are illustrated in Fig 10B. Since the scalloping extended over a sector of 10°, 100 feet of fence on the west side and 150 feet on the east side were replaced with a wooden picket fence. The scalloping was then reduced to a negligible magnitude

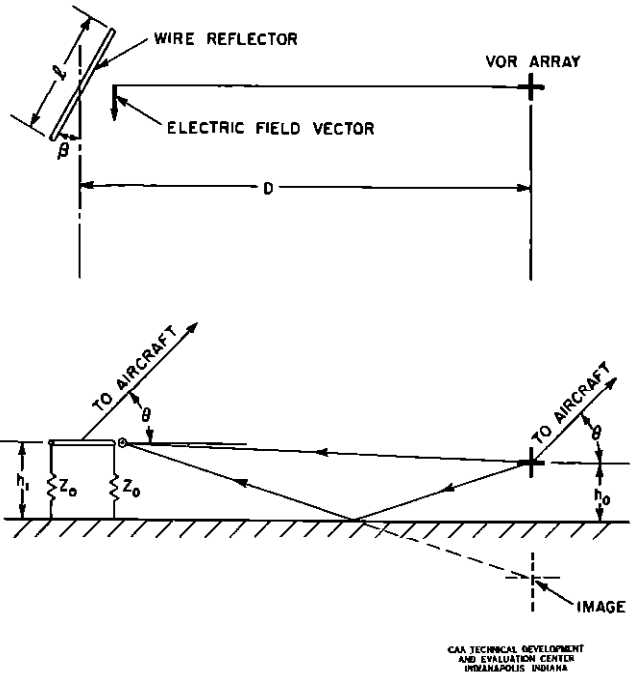


Fig. 11 A Wire Reflector Located Near a VOR

THEORETICAL CONSIDERATIONS

A general solution to the wire reflection problem appears to be a tremendous undertaking, however, some understanding of the phenomena may be obtained by approximate approaches to the problem. Fig 11 presents the arrangement of the reflector with respect to the VOR. From this the relative magnitude of the error to the VOR caused by a wire may be derived as follows.

The field intensity in the vicinity of the wire is expressed by

$$E = \frac{K_1}{D} \sin\left(\frac{2\pi}{\lambda} \frac{h_0 h_1}{D}\right) \tag{1}$$

where λ is the wavelength and K_1 is a constant. This expression assumes a perfectly conducting earth for horizontal polarization. In practice this assumption is true to a first approximation, particularly for small reflection angles. The wire is assumed to be terminated in its characteristic impedance Z_0 at both ends. Hence, the current produced in the wire by the electric field is

$$I = \frac{E l \cos \beta}{2 Z_0} \tag{2}$$

where l , the wire length, is assumed to be small so that the induced incremental voltages are in phase throughout the length of the wire and may be added algebraically

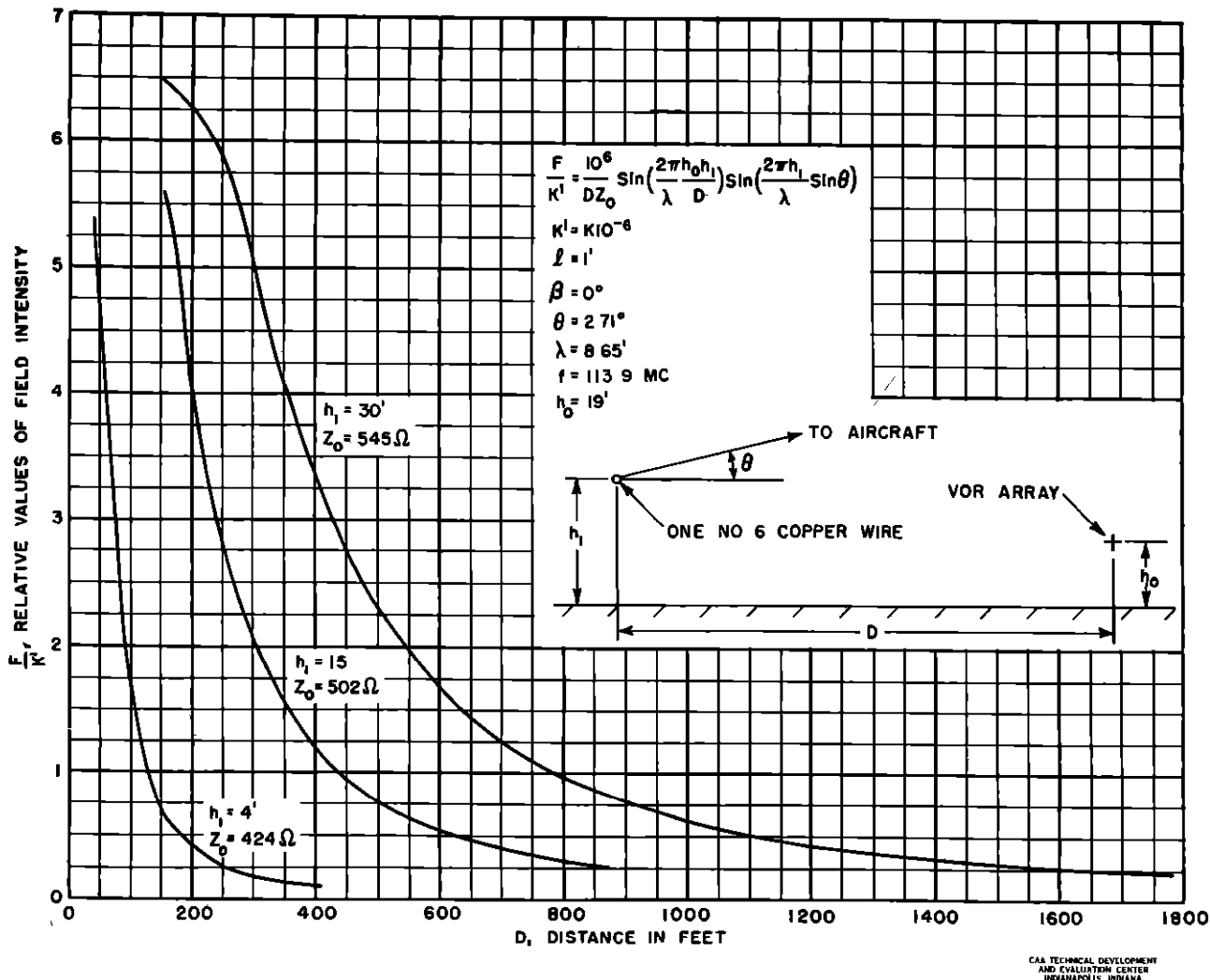


Fig. 12 Theoretical Field Intensity in Vicinity of Aircraft Due to Reflection From Wire

The horizontally polarized field radiated by the wire in a given azimuthal direction is

$$F = K_2 I \sin\left(\frac{2\pi h_1}{\lambda} \sin\theta\right) \quad (3)$$

where K_2 is a constant and θ is the elevation angle of transmission from the wire to the aircraft. Equation (3) holds for vertical polarization as well as for horizontal polarization for small values of θ over land. Combining Equations (1), (2), and (3)

$$\frac{F}{K} = \frac{l \cos\beta}{D Z_0} \sin\left(\frac{2\pi}{\lambda} \frac{h_0 h_1}{D}\right) \sin\left(\frac{2\pi h_1}{\lambda} \sin\theta\right) \quad (4)$$

Equation (4) is shown plotted in Fig. 12 for several of the parameters tested.

The omnibearing deviation indicator error caused by the wire is directly pro-

portional to the field intensity radiated by the wire. The data in Table II shows how the measured error varied with distance as compared with the equalized data calculated by means of Equation (4). Since Equation (4) applies to short wires, the calculated errors are approximate only, whereas long wires were used in the tests.

If only the characteristic impedance is varied, using Equation (4), the following equation results

$$\frac{F'}{F} = \frac{Z_0}{Z_0'} \quad (5)$$

where the prime indicates a new field in the vicinity of the aircraft because of a new value of characteristic impedance. One No. 6 conductor 30 feet above ground has a characteristic impedance $Z_0 = 545$ ohms. For two

TABLE II

Measured Scalloping Amplitude Compared to Predicted Scalloping Amplitude

Test Conditions	Azimuth (Degrees)	D (Feet)	h_1 (Feet)	Over-all Error Due to Wires (Degrees)	
				Measured	Theoretical, from Fig 12
Fig 4	50	203	30	5 15	5 15*
Indianapolis VOR	310	1630	30	0 25-0 37	0 207*

* Equalized with measured 5.15°

No. 6 conductors spaced 12 inches apart horizontally, $Z'_0 = 394$ ohms. Hence,

$$\frac{F'}{F} = \frac{545}{394} = 1.38$$

The measured ratio was 1.56

Equation (5) is a tool useful in estimating the effect of a number of conductors with various spacings. It is interesting to note that if two conductors of No. 6 solid copper are placed side by side and touching, $Z'_0 = 524$ ohms and

$$\frac{F'}{F} = \frac{545}{524} = 1.04$$

Such a change would be difficult to measure.

A fence is considered as a special case, where the wire is close to the ground. A height of four feet has been used as an average fence height. In Fig 12, the equation $h_1 = 4$ feet is representative of a fence. The topmost wire on a fence is the most detrimental, and is used to represent the fence as an approximate solution. The effect of all the wires may be included by finding the characteristic impedance of the system of wires, then by using a height h_1 somewhere between midheight and top of the fence. A study of Fig. 12 shows that a fence, $h_1 = 4$ feet, will cause scalloping as much as that caused by power lines, provided the fence is fewer than 130 feet from the VOR array. This distance is based on the fact that a power line 800 feet distant and 30 feet high causes scalloping of 1.5° total spread (measured on a 20-mile radius circle). In Fig. 12, $h_1 = 4$ feet indicates that very severe scalloping may be caused by a fence located 50 to 100 feet away from the VOR array.

The frequency of the scalloping will be low, since the fence must be located close to the VOR to produce measurable amplitudes. Equation (13) gives the frequency of the scalloping

Fig 13 is a curve (derived theoretically) which shows how the amplitude of

scalloping varies from a nondirectional reflector with azimuth of the receiver. This information may be used to predict the relative amplitude of the scalloping produced by a plane reflecting surface, if we assume that the reflecting object is located in the place of the nondirectional reflector of Fig 13 and if the surface is turned as the

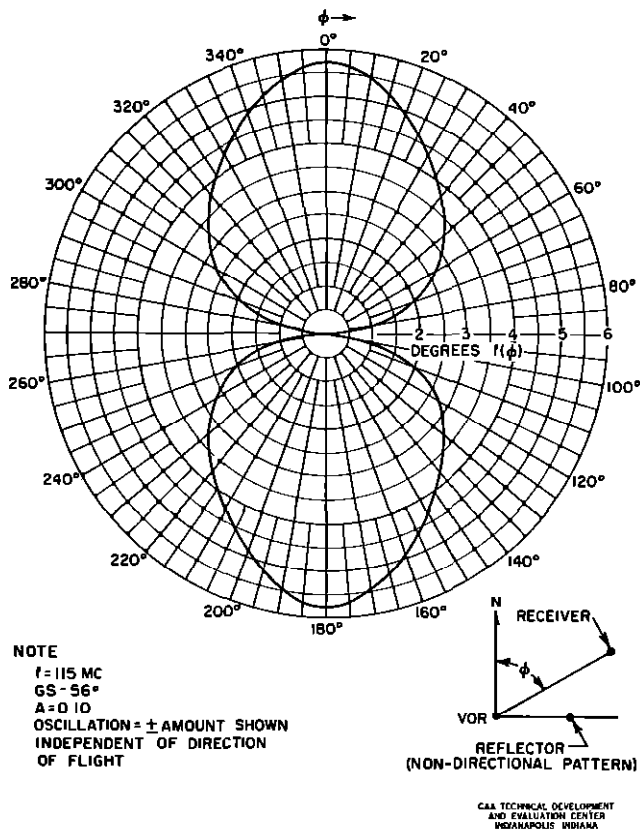
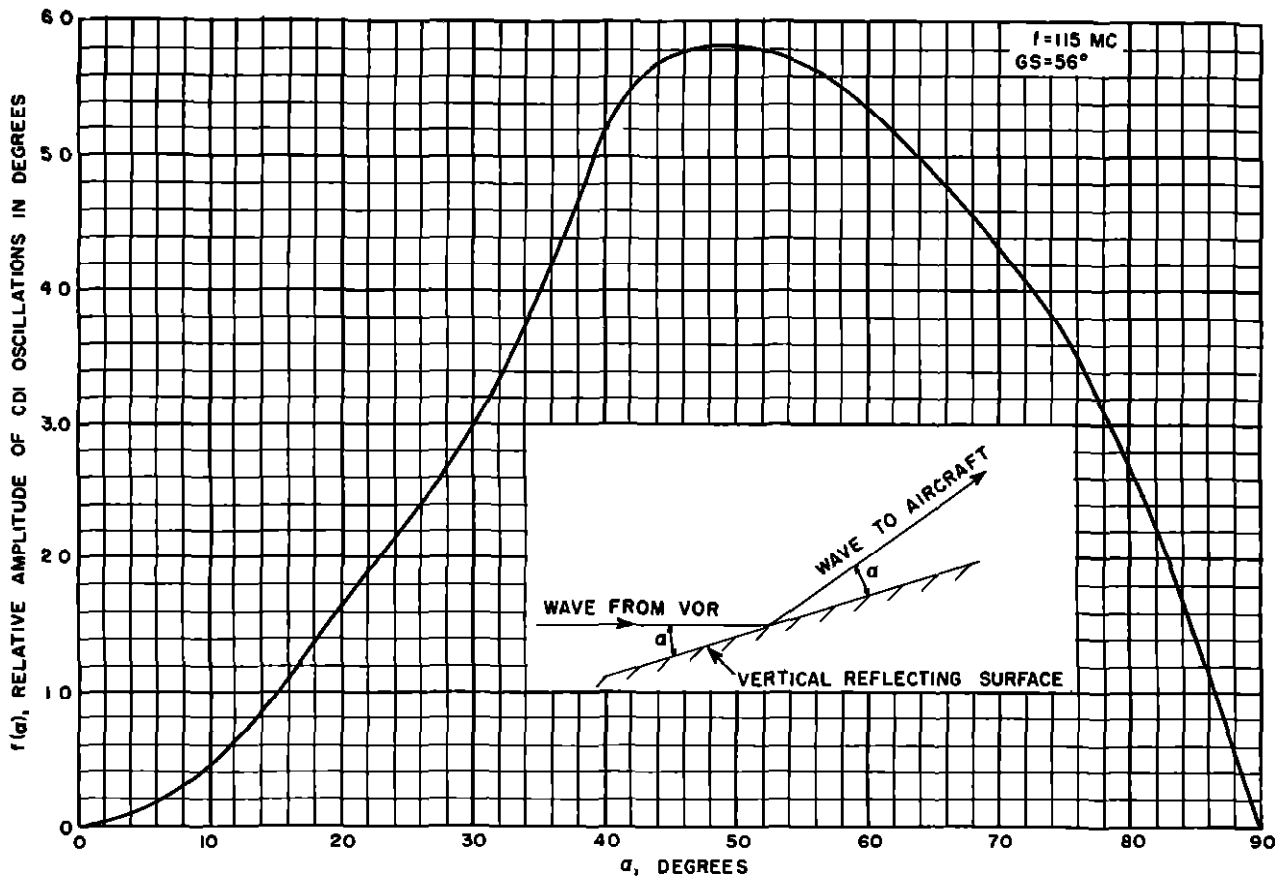


Fig. 13 Amplitude of Cross Pointer Oscillations Due to One Reflecting Object Versus Azimuth Angle (Oscillation = ± Amount Shown) (Independent of Direction of Flight)



CAA TECHNICAL DEVELOPMENT
AND EVALUATION CENTER
INDIANAPOLIS, INDIANA

Fig. 14 Amplitude of Course Deviation Indicator Oscillations Caused by an Optical Reflection From a Vertical Plane Surface Versus Reflection Angle

aircraft circles the station so that the reflected wave goes to the aircraft. The field intensity of the reflected wave will be proportional to the area normal to the arriving wave. This may be expressed more clearly by using Equation (6) to aid in obtaining the curve of Fig. 14.

$$f(\alpha) = 1.416 f(\phi) \sin \alpha \quad (6)$$

where α is obtained from the geometry or from the expression

$$\alpha = 45^\circ - \frac{\phi}{2} \quad (7)$$

$f(\alpha)$ is the amplitude of the curve of Fig. 14.

$f(\phi)$ is the amplitude of the curve of Fig. 13.

Fig. 14 may be used to predict the amount of scalloping produced by each small section of a horizontal straight wire or any other object such as a vertical hangar face.

Equation (1) is used to express the di-

rect field in the vicinity of the aircraft. Equation (4) with the cosine term omitted, since $f(\alpha)$ takes it into account, is a statement of the reflected field, and $f(\alpha)$ from Fig. 14 accounts for the difference in azimuth of the aircraft and the reflecting object.

Then using Equations (1) and (4) and Fig. 14

$$S = \frac{K_3 D_1 f(\alpha) \sin\left(\frac{2\pi}{\lambda} \frac{h_0 h_1}{D}\right) \sin\left(\frac{2\pi h_1}{\lambda} \sin \theta\right)}{D_1 D \sin\left(\frac{2\pi h_0}{\lambda} \sin \theta\right)} \quad (8)$$

where

S = amplitude of scalloping

D_1 = distance from reflector to aircraft

D_2 = distance from VOR to aircraft

K_3 = a constant depending upon the reflector size and other parameters

Since Z_0 changes so little with height h_1 , it is taken as a constant and combined with K_3 . The value of S is determined by a flight test. Another small section of the same (or similar) reflector will then produce scalloping expressed by

$$S = \frac{K_3 D_2 f(a) \sin\left(\frac{2\pi}{\lambda} \frac{h_0 h_1'}{D}\right) \sin\left(\frac{2\pi h_1'}{\lambda} \sin\theta\right)}{D_1 D \sin\left(\frac{2\pi h_0}{\lambda} \sin\theta\right)} \quad (9)$$

Combining Equations (8) and (9)

$$S' = S \left[\frac{D_2 f(a) \sin\left(\frac{2\pi}{\lambda} \frac{h_0 h_1'}{D}\right) \sin\left(\frac{2\pi h_1'}{\lambda} \sin\theta\right)}{D_1 D \sin\left(\frac{2\pi h_0}{\lambda} \sin\theta\right)} \right] \quad (10)$$

$$S' = S \left[\frac{D_2 f(a) \sin\left(\frac{2\pi}{\lambda} \frac{h_0 h_1'}{D}\right) \sin\left(\frac{2\pi h_1'}{\lambda} \sin\theta\right)}{D_1 D \sin\left(\frac{2\pi h_0}{\lambda} \sin\theta\right)} \right]$$

If the aircraft is at the same distance and elevation angle from the reflector and the VOR for both cases, Equation (10) is simplified and becomes

$$S' = S \left[\frac{D f(a) \sin\left(\frac{2\pi}{\lambda} \frac{h_0 h_1'}{D}\right) \sin\left(\frac{2\pi h_1'}{\lambda} \sin\theta\right)}{D f(a) \sin\left(\frac{2\pi}{\lambda} \frac{h_0 h_1'}{D}\right) \sin\left(\frac{2\pi h_1'}{\lambda} \sin\theta\right)} \right] \quad (11)$$

A great simplification can be made in Equation (11) if

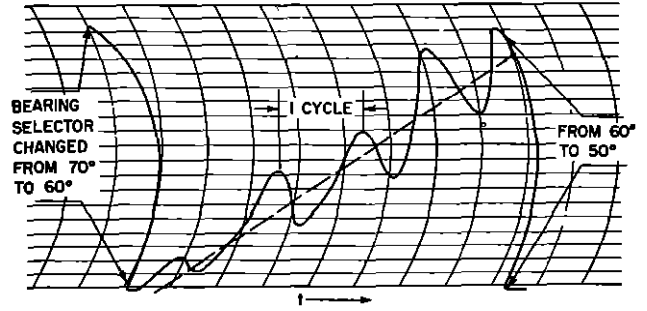
$$\frac{h_0 h_1'}{D} \leq 107 \text{ FEET}, \quad \frac{h_0 h_1}{D} \leq 107 \text{ FEET},$$

$$h_1' \sin\theta \leq 107 \text{ FEET}, \quad \text{AND } h_1 \sin\theta \leq 107 \text{ FEET}$$

This simplification admits an error of 11 per cent or less for each sine term. Equation (11) then becomes

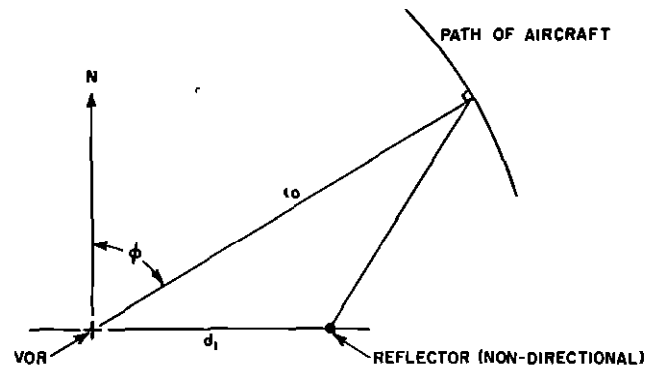
$$S' = S \left(\frac{D h_1'}{D' h_1} \right)^2 \left(\frac{f(a)}{f(a)} \right) \quad (12)$$

Equation (8) indicates how the scalloping from a horizontal wire or vertical plane surface varies. One of the Equations (10),



CAA TECHNICAL DEVELOPMENT AND EVALUATION CENTER INDIANAPOLIS, INDIANA

A. Sample Recording Showing One Cycle of Course Deviation Indicator Oscillation



CAA TECHNICAL DEVELOPMENT AND EVALUATION CENTER INDIANAPOLIS, INDIANA

B. A VOR and One Reflecting Object

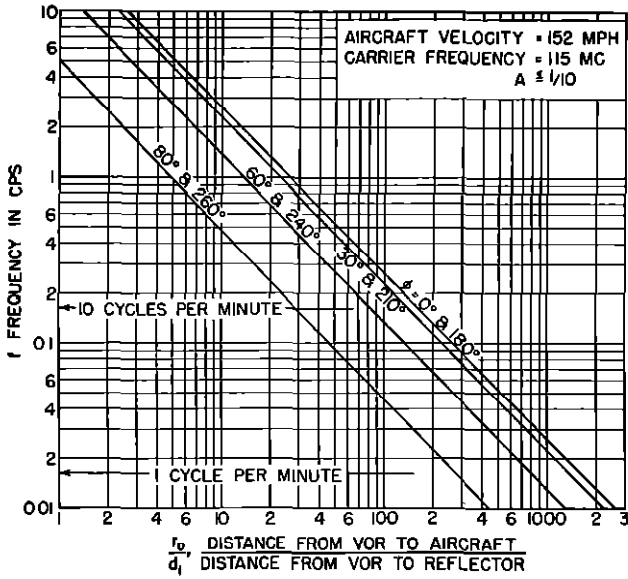
Fig. 15 Figures Concerned With VOR Course Scalloping

(11), or (12), whichever is most applicable, may be used to predict the amplitude of scalloping S' , if the amplitude of scalloping S for one set of conditions is known

Fig. 15A represents a sample recording of the course deviation indicator taken when the aircraft was flying around the VOR. The dashed straight line is the path which the recorder pen would have followed had no reflecting object been present. The errors introduced by wires show up as a periodic variation about the correct bearings received directly from the VOR. In Appendix I of this report, the following equation was derived for the frequency of the oscillation in cps

$$f = N \left[\frac{\cos\phi}{\sqrt{\left(\frac{r_0}{d_1}\right)^2 + 1 - 2\left(\frac{r_0}{d_1}\right) \sin\phi}} \right] \quad (13)$$

where N is the velocity of the aircraft in wavelengths per second and the other symbols are defined in Fig. 15B. Fig. 16 is a plot of

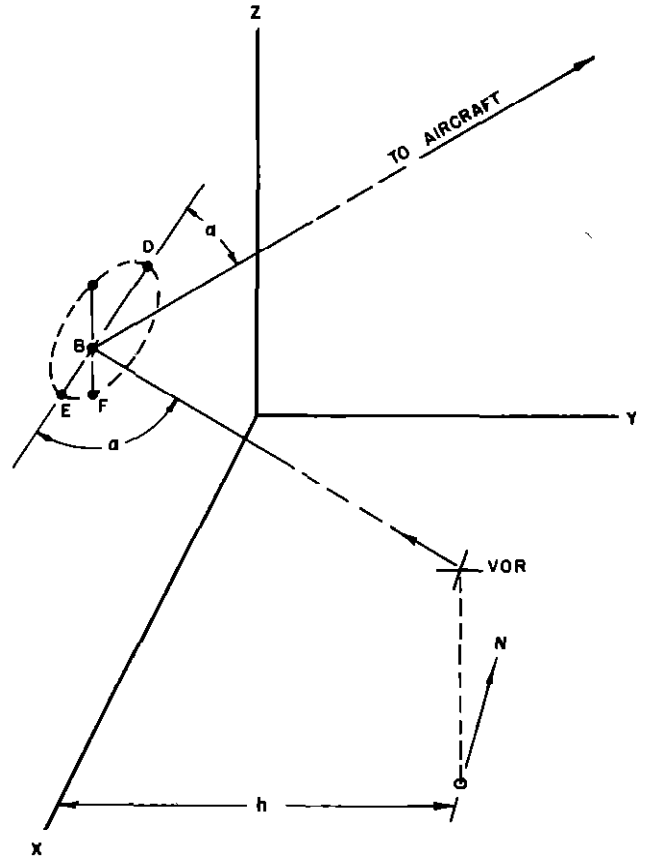


CAA TECHNICAL DEVELOPMENT AND EVALUATION CENTER INDIANAPOLIS INDIANA

Fig. 16 Omnirange Course Scalping Frequency For Cross-Course Flights

Equation (13) with ϕ as the parameter. Assume $f = 115$ megacycles (MC) and aircraft speed = 152 mph. Then $N = 26.05$ wavelengths per second. Equation (13) makes possible a determination of the frequency of the oscillation caused by wires, independent of amplitude. Table III shows measured calculated values for Fig 4 and for another example, the commissioned VOR at Indianapolis, Indiana.

Fig. 17 represents a VOR with a vertical reflecting surface located at a distance



CAA TECHNICAL DEVELOPMENT AND EVALUATION CENTER INDIANAPOLIS INDIANA

Fig. 17 The Fresnel First Zone of a Vertical Sheet Reflector

h , due west. The elliptical figure (shown dashed) indicates the Fresnel first zone located in the vertical reflecting surface.

TABLE III

Measured Scalping Frequency Compared to Predicted Scalping Frequency

Test Conditions	Azimuth (Degrees)	r_0 (Miles)	d_1 (Miles)	ϕ (Degrees)	Measured	Calculated (Frequency cps)	Comments
Fig. 4	50	15	0.0384	20	0.0833	0.063	Center of north half of wire taken as source of reflected wave.
Fig. 4	60	15	0.0384	30	0.0584	0.061	
Indianapolis VOR	310	6	0.308	10	1.4	1.41	Point of optical reflection of wire to aircraft taken as source of reflected wave

$f = 115$ MC
Aircraft speed = 160 mph

The wave which reflects from the vertical surface at point B does so by inducing currents in the surface. The currents contained in the Fresnel first zone produce the reflected wave. The zones outside of the first cancel each other's effects, making the first zone the only part of the area required to bring about a complete reflection. A discussion of the first Fresnel zone may be found in a paper¹ by Hey, Parsons, and Jackson of the British Ministry of Supply. The equations which follow give approximately the dimensions of the first Fresnel Zone

$$BD = \frac{\lambda \cos \alpha + \sqrt{\lambda^2 \cos^2 \alpha + 4h\lambda \sin \alpha}}{2 \sin^2 \alpha} \quad (14)$$

$$BE = \frac{-\lambda \cos \alpha + \sqrt{\lambda^2 \cos^2 \alpha + 4h\lambda \sin \alpha}}{2 \sin^2 \alpha} \quad (15)$$

$$BF = \sqrt{\frac{h\lambda}{\sin \alpha}} \quad (16)$$

where λ = wavelength, and Fig 17 defines the remaining symbols

If it is assumed that a vertical sheet that conducts well includes the wire of Fig. 6, then the dimensions of the Fresnel first zone are found as follows for the assumed point of reflection, the midpoint of the wire $\lambda = 8.56$ feet, $h = 177$ feet, and

¹J. S. Hey, S. J. Parsons, and F. Jackson, "Reflexions of Centimetric Electromagnetic Waves Over Ground, and Diffraction Effects with Wire-Netting Screens," Proceedings of the Physical Society, London, Vol. 59, pp. 847-857, September 1, 1947.

$\alpha = 60.55^\circ$ Then $BE = 45.1$ feet, $ED = 95.7$ feet, and $BF = 41.7$ feet.

This explains why the wire length had little effect in the 50° , 60° , and 70° directions, as in Figs 1 and 4 for example. A horizontal wire meets the requirement for the DE dimension but, of course, fails for the vertical height required, viz, $2BF$.

The wire reflectors shown in Figs 1 to 9 produce a radiation pattern which is symmetrical about the wire. Yet all of the tests, Figs. 1 to 9, showed no measurable error caused by the wire on the wire side of the VOR. The wire radiates in the directions 330° , 320° , and 310° azimuth as shown by the dashed lobe in Fig 8. It is believed that the 30-cps phase angle transmitted by the wire is within approximately 10° of the 30-cps phase angle transmitted directly to the aircraft from the VOR or 180° from this value, because the wire lies in the 315° to 335° azimuth sector. Therefore, the error in the 310° to 330° azimuth sector caused by the wire would be zero or so small that it would be difficult to measure.

CONCLUSIONS

It has been shown that errors in the form of course deviation indicator oscillations can be caused by wires located near a VOR. A number of examples are given to show what errors can be expected. Equations are included which permit an estimate of the frequency of the error as well as its relative magnitude. The error increases as the number of conductors is increased, being inversely proportional to the characteristic impedance of the wire system. Radial wires cause no measurable error. The wave appears to reflect from the wire according to geometrical optics, and therefore a wire acts very much like a vertical reflecting sheet containing the wire.

APPENDIX I

OMNIRANGE COURSE SCALLOPING*

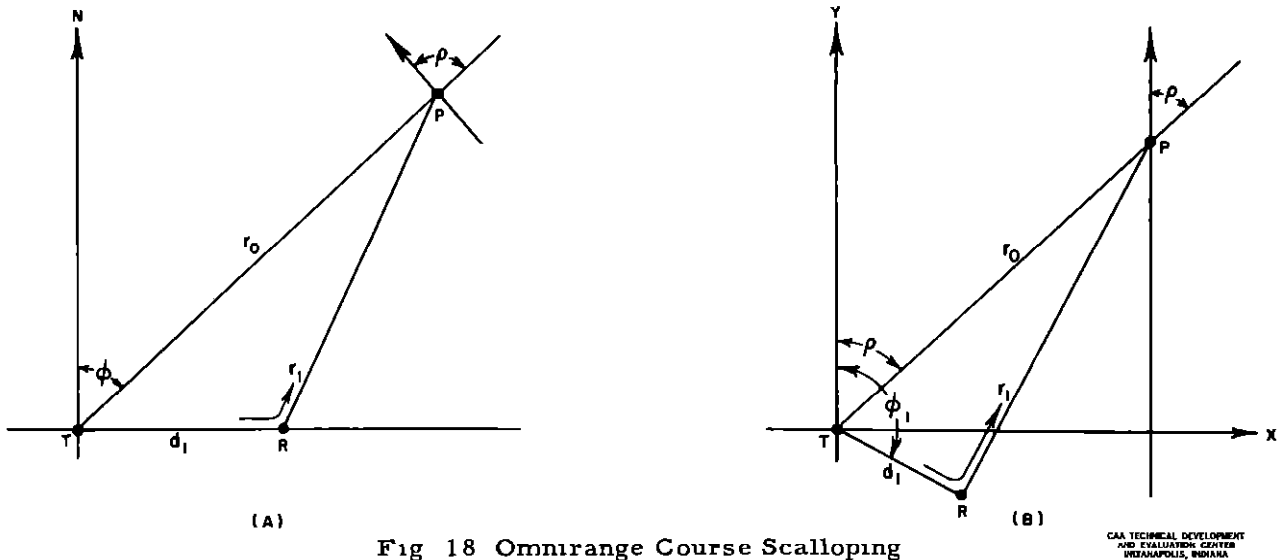


Fig 18 Omnirange Course Scalping

The course scalloping of omnirange courses treated in this appendix is that caused by reflections of electromagnetic energy from objects located both close to and remote from the omnirange. The problem in general is very complicated because of the many variables encountered. However, much is to be learned about course scalloping phenomena by considering the simplest possible case, that of one reflecting object. A complex course scalloping problem may be solved by treating its parts one at a time and combining their effects in a proper manner.

In this study no attempt is made to solve the re-radiation characteristics of various objects, herein, it is assumed that the phase change upon reflection is δ and that the amount of voltage at the receiver input due to the reflected wave is A times as much as the voltage appearing at the receiver due to the direct wave. The re-radiating object is assumed to radiate equally well in all directions. The advantage of making the above assumptions is that the results of reflections from objects, as

observed in aircraft, are obtained with a minimum of effort.

Since the omnirange radiates energy equally in all directions, we are at liberty to locate the reflecting object in any direction. The location of the reflector has been arbitrarily chosen as 90° azimuth with respect to the range for all curves shown in this appendix. Fig 18 presents the arrangement of the problem, and Fig 18A applies to all the attached curves. Referring to Fig 18A, T represents the omnirange, R the re-radiating object, and P the receiving aircraft. The arrow at P indicates the direction of flight. The azimuth of the aircraft is ϕ , and ρ is its direction of flight with respect to the course.

A study of the problem of reflection indicates that, at the receiving aircraft, two pairs of variable phase sidebands are received, one pair is in phase with the carrier, the other is in phase quadrature with respect to the carrier. The effects produced in the receiver output by the phase quadrature sidebands depend upon the characteristics of the receiving equipment and will not be considered here. The in-phase sidebands plus the carrier constitute an amplitude modulated wave which produces the variable phase output of the receiver. It is this output with which we are concerned, for the phase of the variable phase output signal determines the location of the omnirange course selected.

It is shown in Appendix II that the

* The material for the Appendices I, II, and III was taken from a previously unpublished memorandum by S R Anderson, CAA Experimental Station, May 14, 1945

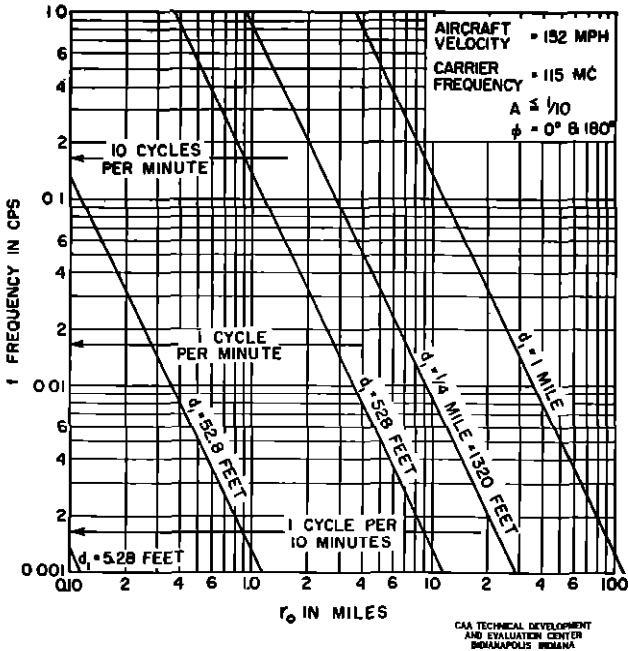


Fig. 19 Omnirange Course Scalloping Frequency For Radial Flights

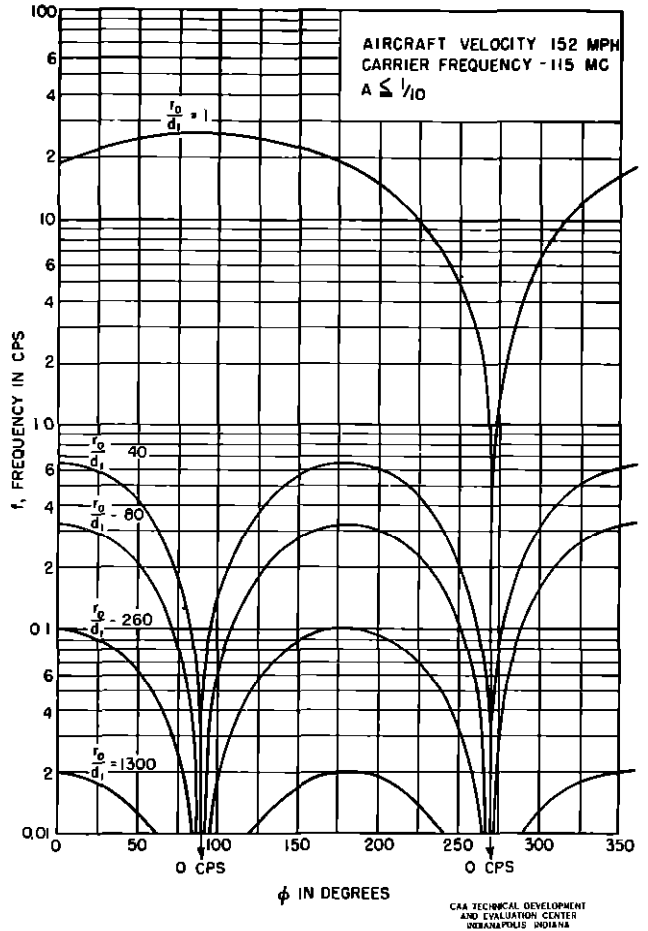


Fig. 20 Omnirange Course Scalloping Frequency For Cross-Course Flights

phase of the variable phase signal varies between

$$\tan^{-1} \left[\frac{\sin(GS \sin \phi)}{\sin(GS \cos \phi)} + \frac{A \sin GS}{\sin(GS \cos \phi)} \right]$$

and

$$\tan^{-1} \left[\frac{\sin(GS \sin \phi)}{\sin(GS \cos \phi)} - \frac{A \sin GS}{\sin(GS \cos \phi)} \right]$$

This is due to the reflection of energy from one object. The swing of the phase angle of the variable phase voltage is equal to the number of degrees of swing of the omnirange course. The magnitude of the course distortion is dependent upon A. The frequency of the course swing (course scalloping) is given in Appendix III. It is the frequency of the course scalloping with which this treatment is concerned primarily.

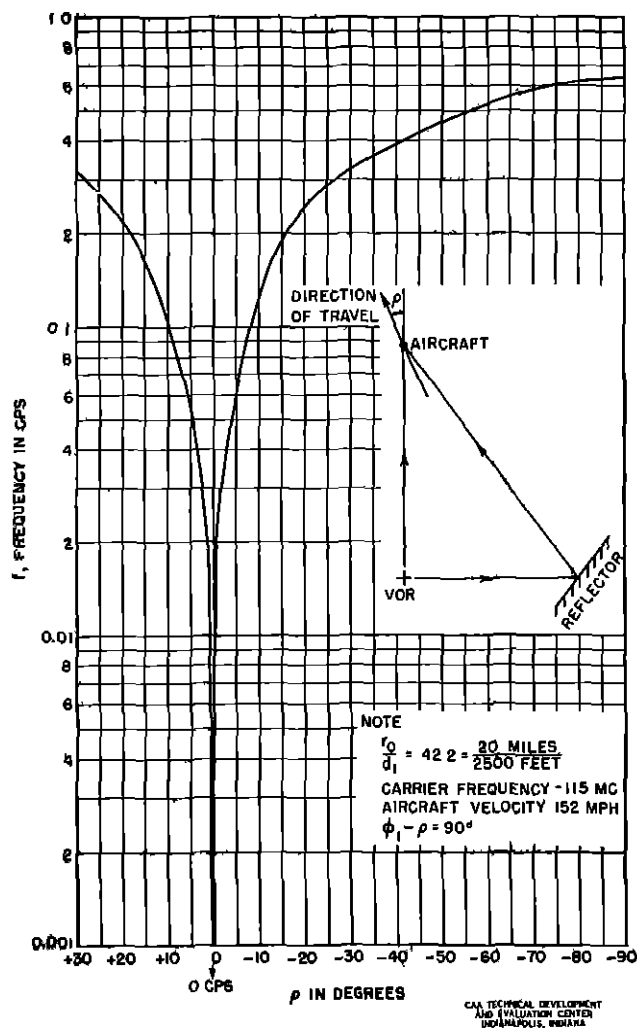
Fig. 19 shows the frequencies of the course distortion for radial flights toward or away from the station at an azimuth of 0° or 180°. The aircraft is located various distances r from the range, while the re-radiating object is at a distance d₁ from the range. It is interesting to note that the frequency increases as the aircraft nears the omnirange, or, holding the aircraft distance constant, the frequency of the course scalloping decreases with a decrease in d₁, which is the distance between the reflector and the range. Because of the

mechanical dampening of the instrument and the 1250-microfarad condenser across the instrument, all frequencies above approximately 1 cps would not appear on the course deviation indicator. All frequencies below approximately 0.0010 cps would appear as a fixed error in the course. Consequently, the various distances of the aircraft and the reflector from the range must be considered when flight testing.

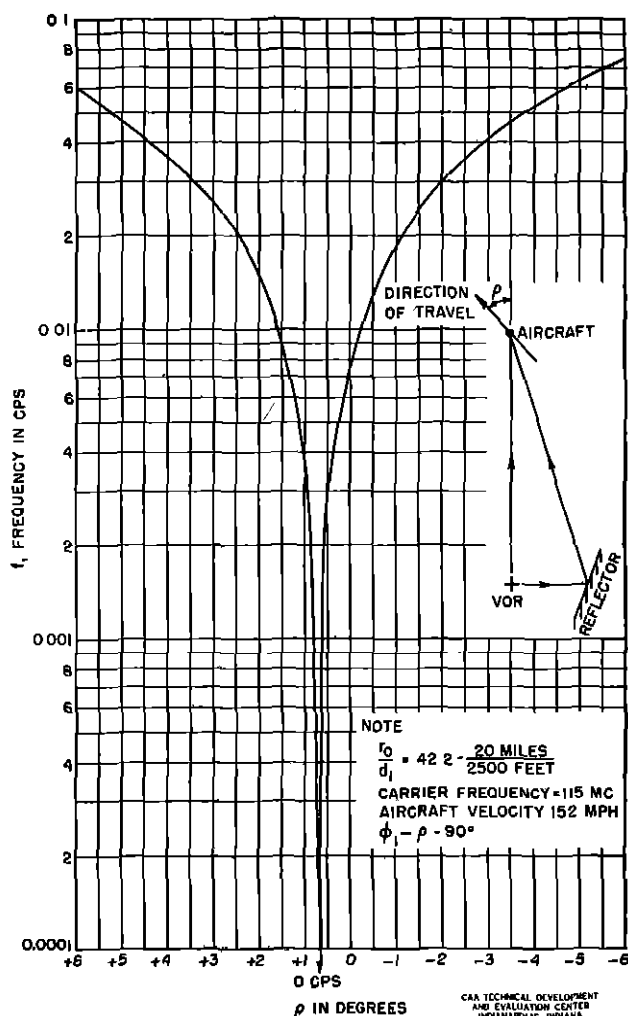
The direction of flight of the aircraft on a given course affects the scalloping frequency. Fig. 20 presents calculated results of a flight circling the range at a fixed radius

r₀ for various values of $\frac{r_0}{d_1}$. It is apparent

that for a given distance from the range station the scalloping frequency is less for a radial flight than for a circular flight. It is also clear that, as the aircraft flies around the station, the frequency of distortion rises to a maximum then drops off to zero when



A. Course Scalping Frequency Versus Direction of Travel of Aircraft



B. Course Distortion Frequency Versus Direction of Travel of Aircraft

Fig. 21 Course Scalping Frequency Versus Direction of Travel of Aircraft

along a line joining the range and reflector. The magnitude of the scalping reduces to zero gradually as the aircraft approaches the 90° and 270° azimuths with respect to the range*. The same information is presented in Fig. 16 when $\phi = 0^\circ$ and 180° , but with $\frac{r}{d_1}$ as the abscissa. For values not given in any of the above curves and for flights other than radial and 90° cross-course flights, one may use the formulae derived in Appendix III.

* This follows from Equation (14), Appendix II.

Figs 21A and 21B show, by means of a typical example, how critical the course scalping frequency is with respect to the direction of travel of the aircraft, when the aircraft is 20 miles from the VOR and the reflector is 2,500 feet from the VOR. Referring to Fig 21A, if the aircraft is flying in a circle with the VOR as a center ($\rho = -90^\circ$) the scalping frequency does not change appreciably with small changes of ρ . The other type of flight check commonly made on a VOR is a radial flight ($\rho = 0^\circ$). Fig. 21A shows that this is a very critical region with regard to the scalping frequency. In Fig 21B, which is a plot of the critical region of Fig. 21A, it is clearly shown that a small change in ρ will cause a large change in the scalping frequency.

Consequently, for flight testing where the scalloping frequency is to be used to determine the source of the scalloping, cross-course flights ($\rho = \pm 90^\circ$) should be made. If maximum amplitude of scalloping is to be determined, a radial flight should be made.

The reason for this is that the frequency of the scalloping on a radial flight is very low, or even zero at times. The filters across the course deviation indicator become ineffective at low frequencies.

APPENDIX II

A DERIVATION OF THE COURSE SCALLOPING EQUATION

$\phi, \phi_1, d_1, r_0, \rho, r_1$, are all shown in Fig. 18.

E_0 = The voltage appearing at the receiver input due to the wave traveling along r_0 .

E_1 = The voltage appearing at the receiver input due to the wave traveling along r_1 .

$$G = \frac{2\pi}{\lambda}$$

λ = Wavelength of the carrier frequency

t = Time.

$\frac{\omega}{2\pi}$ = Variable phase frequency or modulation frequency.

S = Spacing between a sideband antenna and the middle antenna of the omnidirectional array

δ = Phase change of the radio frequency energy due to reflection.

N = Speed of aircraft in wavelengths per second.

f = Frequency of the course scalloping (cps)

B = Variable phase 30-cps phase angle.

$$J = \sqrt{-1}$$

A equals electric field intensity at the aircraft of the wave traveling along r_1 divided by electric field intensity at the aircraft of the wave traveling along r_0 . (This is independent of path length differences.)

ζ is defined by Equation (24).

Referring to Fig. 18A, the voltage appearing at the receiver due to the wave traveling along r_0 is

$$E_0 = \frac{e^{-jGr_0}}{r_0} \left[1 + \sin \omega t \sin(GS \sin \phi) + \cos \omega t \sin(GS \cos \phi) \right] \quad (17)$$

The first term is the carrier, the other terms are the sidebands of the variable

phase signal. The voltage appearing at the receiver input due to the wave traveling along the path r_1 and experiencing a change of phase and magnitude upon reflection at R is

$$E_1 = \frac{Ae^{-j(Gr_1 + \delta)}}{r_1} (\sin \omega t \sin GS + 1) \quad (18)$$

Here, the second term is the carrier and the first term represents the sidebands due to the variable phase signal. The resultant receiver input voltage is

$$E = E_0 + E_1 \quad (19)$$

For values of d_1 , which are small compared to r_0 , the difference between the attenuation terms due to distance are negligible so that

$$\frac{1}{r_1} \approx \frac{1}{r_0} \quad (20)$$

$$E = \frac{e^{-jGr_0}}{r_0} \left[\sin \omega t \sin(GS \sin \phi) + \cos \omega t \sin(GS \cos \phi) + 1 + Ae^{-j[G(r_1 - r_0) + \delta]} + Ae^{-j[G(r_1 - r_0) + \delta]} \sin \omega t \sin GS \right] \quad (21)$$

The first, second, and last terms are sideband terms while the remaining terms comprise the carrier. The carrier may be rewritten

$$\text{CARRIER} = 1 + A \cos[G(r_1 - r_0) + \delta] - JA \sin[G(r_1 - r_0) + \delta] \quad (22)$$

$$\text{CARRIER} = \sqrt{\left(1 + A \cos[G(r_1 - r_0) + \delta]\right)^2 + A^2 \sin^2[G(r_1 - r_0) + \delta]} e^{+j\zeta} \quad (23)$$

$$\text{WHERE } \zeta = -\tan^{-1} \left\{ \frac{A \sin[G(r_1 - r_0) + \delta]}{1 + A \cos[G(r_1 - r_0) + \delta]} \right\} \quad (24)$$

Equation (21) may be rewritten

$$E = \left[\text{SIDE BANDS} + \text{CARRIER} \right] \frac{e^{-j\theta r_0}}{r_0} \quad (25)$$

$$E = \frac{e^{-j(Gr_0 - \zeta)}}{r_0} \left[\text{SIDE BANDS } e^{-j\zeta} + \text{CARRIER } e^{-j\zeta} \right] \quad (26)$$

$$E = \frac{e^{-j(Gr_0 - \zeta)}}{r_0} \left\{ \sin \omega t \sin(GS \sin \phi) e^{-j\zeta} + \cos \omega t \sin(GS \cos \phi) e^{-j\zeta} \right. \\ \left. + A e^{-j[G(r_1 - r_0) + \delta + \zeta]} \sin \omega t \sin GS + \text{CARRIER } e^{-j\zeta} \right\} \quad (27)$$

In Equation (27) the vector representing the carrier has been turned to the real axis. This enables one to find the in-phase sideband terms by inspection of the following equation.

$$\text{SIDE BANDS} = \left\{ \sin \omega t \sin(GS \sin \phi) \cos \zeta + \cos \omega t \sin(GS \cos \phi) \cos \zeta \right. \\ \left. + A \sin \omega t \sin GS \cos [G(r_1 - r_0) + \delta + \zeta] \right\} \\ - j \left\{ \sin \omega t \sin(GS \sin \phi) \sin \zeta + \cos \omega t \sin(GS \cos \phi) \sin \zeta \right. \\ \left. + A \sin \omega t \sin GS \sin [G(r_1 - r_0) + \delta + \zeta] \right\} \quad (28)$$

The only sideband terms of Equation (28) which combine in the correct phase with the carrier are the real part of Equation (28).

$$\text{IN-PHASE SIDE BANDS} = \left\{ \left[\sin(GS \sin \phi) \cos \zeta + A \sin GS \cos [G(r_1 - r_0) + \delta + \zeta] \right]^2 \right. \\ \left. + \left[\sin(GS \cos \phi) \cos \zeta \right]^2 \right\}^{1/2} \cos(\omega t - \theta) \quad (29)$$

$$\theta = \tan^{-1} \left(\frac{\sin(GS \sin \phi)}{\sin(GS \cos \phi)} + \frac{A \sin GS \cos [G(r_1 - r_0) + \delta + \zeta]}{\sin(GS \cos \phi) \cos \zeta} \right) \quad (30)$$

The first term in the bracket is the normal value for the arc tangent without reflection, because the second term within the brackets goes to zero when A equals zero. Because of reflection the second term may correctly be called the course scalloping term. The value of this term oscillates between a maximum positive value to an equally large negative value as the location of the receiving aircraft changes, that is, $\cos(Gr_1 - Gr_0 + \delta + \zeta)$ varies between -1 and 0, then to +1 as $(Gr_1 - Gr_0 + \delta + \zeta)$ changes. The magnitude of the distortion term varies slowly with a change in ϕ only.

$$A \leq \frac{1}{10}, \quad \cos \zeta = 1 \quad (31)$$

Equation (30) may be rewritten satisfying the two equations in (31).

$$\theta = \tan^{-1} \left(\frac{\sin(GS \sin \phi)}{\sin(GS \cos \phi)} + \frac{A \sin GS \cos [G(r_1 - r_0) + \delta + \zeta]}{\sin(GS \cos \phi)} \right) \quad (32)$$

APPENDIX III

A DERIVATION OF EXPRESSIONS

GIVING THE FREQUENCY OF THE COURSE SCALLOPING

The phase angle B of the variable phase signal changes with a change in the position of the receiving aircraft because of a change in the course scalloping term. This is the second term within the brackets of Equation (32). The rate at which the phase angle B of the variable phase signal changes, with a change in the position of the receiving aircraft, may be obtained by differentiating with respect to the aircraft motion.

This may be done for radial flights as follows

$$f = N \frac{d(r_1 - r_0)}{dr_0}, \frac{d(\delta + \zeta)}{dr_0} \quad 0 \quad \text{FOR } A \leq \frac{1}{10} \quad (33)$$

From the geometry of Fig. 18A

$$r_1 - r_0 = -r_0 + d_1 + \sqrt{r_0^2 + d_1^2 - 2d_1r_0 \sin \phi} \quad (34)$$

$$f = N \left| 1 - \frac{r_0 - d_1 \sin \phi}{\sqrt{r_0^2 + d_1^2 - 2d_1r_0 \sin \phi}} \right| \quad (35)$$

If the aircraft speed is 152 mph, and the carrier frequency 115 MC, then

$$N = 26.05 \frac{\text{wavelengths}}{\text{seconds}}$$

$$f = 26.05 \left| 1 - \frac{r_0 - d_1 \sin \phi}{\sqrt{r_0^2 + d_1^2 - 2d_1r_0 \sin \phi}} \right| = 26.05 \left| 1 - \frac{1 - \frac{d_1}{r_0} \sin \phi}{\sqrt{1 + \left(\frac{d_1}{r_0}\right)^2 - 2\frac{d_1}{r_0} \sin \phi}} \right| \quad (36)$$

If a flight around the range is made at a fixed radius, $\rho = 90^\circ$, the value of f may be found as follows

$$f = N \frac{d(r_1 - r_0)}{r_0 d\phi}, \frac{d(\delta + \zeta)}{d\phi} = 0 \quad \text{FOR } A \leq \frac{1}{10} \quad (37)$$

$$f = 26.05 \left| \frac{\cos \phi}{\sqrt{\left(\frac{r_0}{d_1}\right)^2 + 1 - 2\frac{r_0}{d_1} \sin \phi}} \right| \quad (38)$$

The frequency f of the course scalloping for any direction of flight across course may be determined by considering Fig. 18B. Here the aircraft is assumed to fly parallel to the Y axis. This gives the same results as if the reflector were fixed and the aircraft crossed the course at an angle ρ .

$$f = N \frac{d(r_1 - r_0)}{dy} \quad A \leq \frac{1}{10} \quad (39)$$

$$r_1 - r_0 = d_1 + \sqrt{d_1^2 + x^2 + y^2 - 2d_1(y \cos \phi_1 + x \sin \phi_1)} - \sqrt{x^2 + y^2} \quad (40)$$

$$f = 26.05 \left| \frac{r_0 \cos \rho - d_1 \cos \phi_1}{\sqrt{d_1^2 + r_0^2 - 2d_1r_0 \cos(\phi_1 - \rho)}} - \cos \rho \right| \quad (41)$$

If $\phi_1 - \rho = 90^\circ$, the reflecting object is always at right angles to the course crossed by the aircraft.

$$f = 26.05 \left| \cos \rho - \frac{\frac{r_0}{d_1} \cos \rho + \sin \rho}{\sqrt{1 + \left(\frac{r_0}{d_1}\right)^2}} \right| \quad (42)$$

For accurate calculations where $\frac{d_1}{r_0} > 1$, the following expansion will be found useful

$$\left[1 + \left(\frac{d_1}{r_0}\right)^2 \right]^{-1/2} = 1 + \frac{1}{2} \left(\frac{d_1}{r_0}\right)^2 \left[-1 + \frac{3}{4} \left(\frac{d_1}{r_0}\right)^2 - \frac{5}{8} \left(\frac{d_1}{r_0}\right)^4 + \dots \right] \quad (43)$$